Analysis and Comparison of Different Input Current Control Schemes for a Three-Phase/Switch/Level Boost-Type PWM (VIENNA) Rectifier

Uwe Drofenik, Ron Windauer*, Johann W. Kolar*, E. Masada and Franz C. Zach

The University of Tokyo, Department of Electrical Engineering,
Masada Laboratory
7-3-1, Hongo Bunkyo-ku, Tokyo 113, JAPAN
e-mail: drofenik@masada.t.u-tokyo.ac.jp

* Technical University Vienna, Power Electronics Section 359.5
Gußhausstraße 27, Vienna A-1040, Austria/Europe
Tel.: +43-1-58801-3833 Fax.: +43-1-5058870
e-mail: windauer@ps1.iaee.tuwien.ac.at, kolar@ps1.iaee.tuwien.ac.at

ABSTRACT - For a new three-phase/switch/level boost-type unity power factor PWM rectifier (VIENNA Rectifier) different control schemes for the control of the input current and/or the input voltage are discussed and compared to each other. A simple hysteresis control, a ramp comparison control and a space vector based harmonic-optimal control scheme are analyzed. The comparison of the control concepts is based on equal switching losses. The normalized rms-value of the ripple of the input current and the amplitudes of harmonics with switching frequency are used as quality indices of the assessment. The analysis is performed via computer simulations and analytical calculations. For low modulation indices the space vector based control scheme and the ramp comparison control show advantages concerning the rms-values of the input current ripple as compared to a simple hysteresis control. For higher modulation indices, i.e. for the preferred operating region of the system, the hysteresis control shows surprisingly low harmonic losses which are even lower than for optimal space vector control (with constant switching frequency). However, as a drawback of the hysteresis control a wider distribution of the harmonics with switching frequency has to be taken into account for dimensioning of a main side EMC-filter. Concerning a practical realization of the rectifier system, this paper facilitates the selection of the harmonic optimal control scheme for a specific application and also the design of the input inductances. In addition to these considerations, which are mainly restricted to the AC side of the system, also the effects of the different control schemes on the stress on the output capacitors is analyzed. Finally, the possibilities for including the control of the potential of the output voltage center point into the different control schemes are discussed.

INTRODUCTION

Due to new guidelines, recommendations and regulations (IEEE-519 and IEC-555/IEC-1000-3-2) stating a limitation of the harmonic stress on the mains of power electronic systems, the development of converter concepts with low harmonics of the input currents becomes increasingly important.

In [1], a three-phase/switch/level PWM rectifier system with low effects on the mains has been proposed. Compared to conventional three-phase/six-switch/two level PWM rectifier systems it shows the following advantages:

+ lower level of the harmonics of the mains current with switching frequency
+ lower blocking voltage stress on the power semiconductor devices
+ reduced number of turn-off power semiconductors.

Neglecting the switching overvoltages, all valves of the rectifier have to sustain only the stress of half the output voltage. This makes the use of fast switching devices (power MOSFETs) possible. The three-level characteristic results in a reduced ripple of the approximately sinusoidal input currents compared to a rectifier with a two-level characteristic. This means that compared to a two-level system for a given switching frequency and a given ripple (harmonic rms value of the input currents) the inductance of the input inductances can be decreased and/or the system power density can be increased.

A lot of different control concepts for rectifier systems have been proposed in the past. Their influence on the ripple of the input currents, the spectrum of the input currents, the losses and the stresses on the components are different. There are also big differences in the efforts necessary for realizing the different control concepts. This makes the decision for a certain control concept often difficult. Comparing common control concepts this paper tries to facilitate a decision for the best control concept.

In this paper three frequently used control concepts are applied to a new three-phase/switch/level PWM (VIENNA) rectifier. There, the influences on the mains resulting for the different control methods are analyzed, the ripples and the spectra of the input currents are compared to each other on the basis of equal switching losses. It is necessary to base the comparison on equal switching losses because raising the switching frequency results on one hand in a reduction of the ripple of the input currents, but on the other hand in increased energy losses of the system.

The three control concepts being analyzed are the hysteresis control (also frequently denoted as bang-bang control or tolerance band control), the ramp comparison control (fixed-frequency control) and optimum space vector control. The space vector control is optimized in order to minimize the harmonic rms value of the input currents. In **section 1** the control concepts and their application to the three-phase/switch/level PWM (VIENNA) rectifier are introduced and explained in short. In **section 2** the harmonic rms values of the input currents, resulting for the three control concepts, are compared to each other. In **section 3** the spectra of the input currents is analyzed. This is necessary because the spectrum of the input currents has a significant influence on the design of the EMC-filter on the input side of the rectifier. Finally in **section 4** also the influence of the three control concepts on the dimensioning of the output capacitors of the rectifier is investigated.

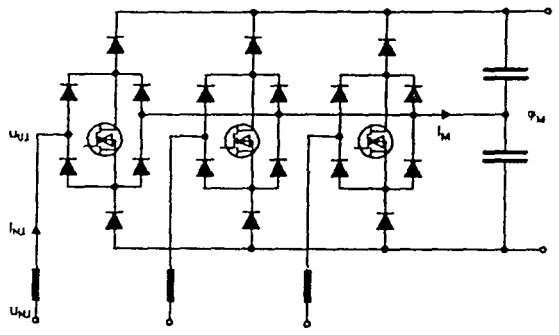

Fig.1: Basic structure of the power circuit of a unidirectional three-phase/switch/level boost-type PWM (VIENNA) rectifier system.

All results given are based on digital simulations of the system under the assumption of an ideal control of the neutral point potential, i.e. a symmetrical distribution of the output voltage of the three-level converter system.

1. BASIC CONSIDERATIONS

1.1 VOLTAGE CONTROL

In order to describe the principle of the operation of the three-phase/level/switch PWM (VIENNA) rectifier it is advantageous to use the space vector calculus. The basic structure of power circuit of the system is shown in **Fig.1**.

With the assumption of a sinusoidal, symmetrical mains voltage system according to a space vector

$$\underline{u}_N = \hat{U}_N e^{j\varphi_N} \quad \varphi_N = \omega_N t \tag{1}$$

(ω_N denotes the mains angular frequency) we have to provide a voltage space vector

$$\underline{u}_U^* = \hat{U}_U^* e^{j\varphi_U} = \hat{U}_N e^{j\varphi_N} - j\omega_N L \underline{i}_N^* \tag{2}$$

in the average over the pulse period T_P at the input of the rectifier system in order to obtain an ideally sinusoidal shape of the mains current

$$\underline{i}_N^* = \hat{I}_N^* e^{j\varphi_N} \tag{3}$$

being in phase with the mains voltage. The voltage space vectors $\underline{u}_U^* = \underline{u}_{U,(1)}$ and $\underline{i}_N^* = \underline{i}_{N,(1)}$ describe the fundamental contributions of the phase quantities.

The space vectors being available for generating the vector $\underline{u}_U^*$ and their allocation to the switching state of the system (s_R, s_S, s_T) are dependent on the sign of the input phase currents. The conditions for $\varphi_N \in (-\pi/6 \ldots +\pi/6)$ and/or $i_{N,R}>0$, $i_{N,S}<0$ and $i_{N,T}<0$ are shown in **Fig.2**. These conditions will be considered as example in the following.

Basically we have at our disposal for the approximation of the continuos motion of $\underline{u}_U^*$ for each combinations of signs of the three-phase currents only 8 out of a total of 19 different space vectors of the system. The vector $\underline{u}_U^*$ therefore can be formed only in the average over a pulse period T_P.

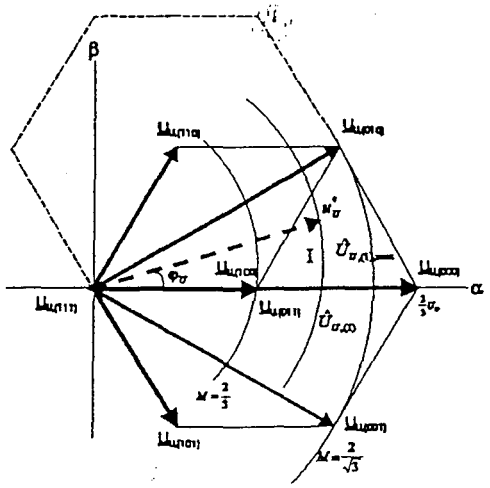

Fig.2: Voltage space vectors $\underline{u}_{U,j}$ which are associated to the switching states and/or to the triple $j=(s_R,s_S,s_T)$ of the phase switching functions of the system for $\varphi_N \in (-\pi/6, +\pi/6)$ and/or $i_{N,R}>0$, $i_{N,S}<0$ and $i_{N,T}<0$.

The modulation index of the pulse width modulation is defined as

$$M = \frac{2\,\hat{U}_U^*}{U_o}. \tag{4}$$

The limit to overmodulation is reached for

$$M_{max} = \frac{2}{\sqrt{3}} \approx 1.15 \tag{5}$$

(equal as for 2-level converter systems). In this paper only the system behavior for the region M=[0.67 ... 1.15] is investigated because this is especially interesting for a practical realization of the system.

There is always the redundancy of two switching states of the system regarding the generation of $\underline{u}_U^*$. In Fig.2 the switching states (100) and (011) lead to the same voltage space vector $\underline{u}_U$ if symmetrical output partial voltages of the system are assumed. Only the sum $\delta_{(100)}+\delta_{(011)}$ of the relative on-times of the redundant switching states can be calculated, but no specific distribution of the on-times of (100) and (011) can be determined. The distribution of the redundant voltage space vectors between begin and end of each pulse half period therefore constitutes a degree of freedom of the modulation method. This degree of freedom can be used to control the potential of the output voltage center point (neutral point) and to optimize the system behavior, as will be shown later.

1.2 HYSTERESIS CONTROL

The hysteresis control is also known as bang-bang control or as tolerance band control.

The basic principle is the following: There is a sinusoidal reference current, where the actual phase current is compared with a tolerance band around the reference current associated with that phase. If the actual current tries to leave the tolerance band, the switch of this phase is activated in a way that the current is forced to return into the tolerance band. Therefore the current is reflected between the two border lines of the tolerance band. Similar action takes place in the other two phases. The switching frequency depends on how fast the current changes. Therefore, the switching frequency is not constant, but varies along the current waveform; it shows a kind of chaotic behavior [2].

Advantages of the hysteresis control:

+ inexpensive and simple realization of the controller (no digital components are required)
+ the current error is limited by the tolerance band.

Problems of the hysteresis control:

– the switching frequency is not constant but varies dependent on time and operating parameters
– low order harmonics of the mains current can appear
– the design of an optimized EMC-filter is difficult
– the potential of the neutral point does not show natural stability.

In [3] the application of the hysteresis control to the VIENNA-rectifier is discussed in detail. The most important results are now presented in short in the following.

Every switching state of the rectifier contributes to a current i_M. For example, if the current of the phase R is positive and the switch R is closed (while the switches S and T are open), the current of the neutral point i_M will be the input current of the phase R. At the same time the input current of the phase R will increase, because the potential $u_{U,R}$ will be connected directly to the neutral point. If the current exceeds the upper limit of the tolerance band, the switch R is opened, the potential of $u_{U,R}$ will be $+U_O/2$, what results in a decrease of the

current. At this time the contribution of the phase R to the neutral point current i_M will be zero.

If the average value of the neutral point current i_M is not zero, the potential of the neutral point will start to drift, what will cause an asymmetry of the voltages of the output capacitors. In case of the hysteresis control this asymmetry of the output voltages results in an increase of the average value of the neutral point current i_M, so that the asymmetry of the output voltages will be further increased. This means that the neutral point is not stable (positive feedback) in case of hysteresis control. Therefore, also for ideal system function an extra control loop controlling the neutral point potential is required.

With regard to section 2 it should be pointed out that the switching frequency is not constant, but can be influenced directly by the width of the tolerance band. For a small width of the band the current error and therefore the harmonic rms value of the input current remains small, but the switching frequency and therefore the switching losses will be relatively high.

1.3 RAMP COMPARISON CONTROL

In the literature the ramp comparison control is also known as fixed-frequency control [4].

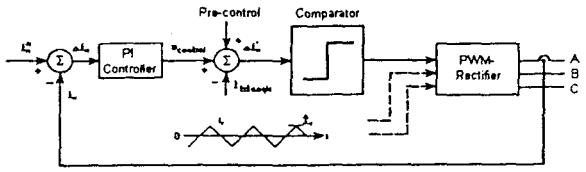

Fig.3: Fixed frequency phase current control.

The current error between the reference current i_N^* and the actual current i_N is added to a fixed-frequency triangular waveform i_T having switching frequency. Whenever the resulting signal $\Delta i_N'$ crosses the zero-line, the switching state of the phase changes. The current error can be interpreted as an offset of the triangular signal, which influences the on- and off-times and/or the duty cycle of the switch. Similar action takes place for the other two phases.

The ramp comparison control shows the following advantages:

+ inexpensive and simple realization of the controller
+ the switching frequency is constant
+ constant switching frequency simplifies the design of an optimized EMC-filter
+ the output voltage center point of the system shows natural stability.

The main disadvantage is:

– the current control error is not limited.

The block diagram of the ramp comparison control is shown for one phase in Fig.3. Besides the above-mentioned structure there is a pre-control signal added to the current error, which is dependent on the input phase voltage u_N according to Eq.(6). This pre-control signal i_P pretends a current error in a way that the controller is forming a voltage u_U according to the input voltage u_N. This results in a significant reduction of the ripple of the input currents.

$$u_N > 0 \quad i_P = \hat{I}_T\left(4\frac{u_N}{U_O} - 1\right) \qquad (6)$$

$$u_N < 0 \quad i_P = \hat{I}_T\left(4\frac{u_N}{U_O} + 1\right)$$

The parameters of the triangular signal are determined according to the following assumptions: Whenever the signal $\Delta i_N'$ crosses the zero-line the switching state is changed. This forces the current to increase or decrease. If the rate of change of the input current is higher than the rate of change of the triangular signal the change of the switching state would make the signal $\Delta i_N'$ to cross the zero-line immediately again and so on. This would result in a switching frequency much higher than the frequency of the triangular signal and the switching losses would be increased significantly. The switching losses would be increased on a large scale.

Therefore it is necessary to make sure that the rate of change of the input current is always smaller than the rate of change of the triangular signal. For determining the critical rate of $\Delta i_N'$ one can assume (as can be confirmed by digital simulation) that the ramp comparison control always selects switching states, that are next to the actual space vector $\underline{u}_N$ of the input voltage. For the vector $\underline{u}_U^* \approx \underline{u}_N$ shown in Fig.2 these are the switching states (000), (010), (011) and (100). According to these assumptions Eq.(7) must be valid for modulation indices M = [0.67 ... 1.15]

$$\hat{I}_T > \frac{U_O}{8\, f_T\, L}. \qquad (7)$$

If M>1 is valid overmodulation occurs. This means that the current error is that high, that the signal Δi, which is the triangular signal plus the current error as an offset, has no zero-crossings within wide sections of the time axis. Therefore the effective switching frequency becomes much lower than the frequency of the triangular signal, what results in reduced losses. This means that the frequency of the triangular signal can be increased, which will increase the effective switching frequency in the sections, where the signal Δi is crossing the zero-line. So the harmonic rms value of the input current is being reduced, but low-frequency harmonics like the 5th, the 7th and so on, are being increased significantly.

Because of this disadvantage the use of the overmodulation is tried to be prevented in rectifier systems. Therefore in this paper the analysis of the overmodulation M>1 of the ramp comparison control was not carried out in more detail.

Compared to the hysteresis control the ramp comparison control shows a stable neutral point potential. This means that an asymmetry of the two output voltages results in an average value of the neutral point current i_M that loads the capacitor showing the lower partial voltage, so that the asymmetry is being reduced to zero. While for hysteresis control a special control loop for the neutral point potential is absolutely necessary, in case of ramp comparison control such an extra control loop is not necessary in principle. But it is, however, of advantage to use such an extra control loop also with the ramp comparison control in order to guarantee a maximum blocking voltage stress on the valves also for changing load state of the system.

For M<1 the effective switching frequency equals the frequency of the triangular signal. With the choice of the frequency of the triangular signal the switching losses can be influenced directly.

1.4 SPACE VECTOR CONTROL

The assumptions in the following section are based on the explanations and equations concerning the space vector calculus in section 1.1.

Basically we have at our disposal for the approximation of the continuos motion of $\underline{u}_U^*$ for each combinations of signs of the three-phase currents only 8 out of a total of 19 different space vectors of the system. The vector $\underline{u}_U^*$ therefore can be formed only in the average over a pulse period T_P. With regard to a best possible approximation one applies only those rectifier voltage space vectors lying in the immediate vicinity of the vector tip of $\underline{u}_U^*$. In Fig.2 these are the space vectors associated to the switching states (000), (010), (011) and (100) and we have

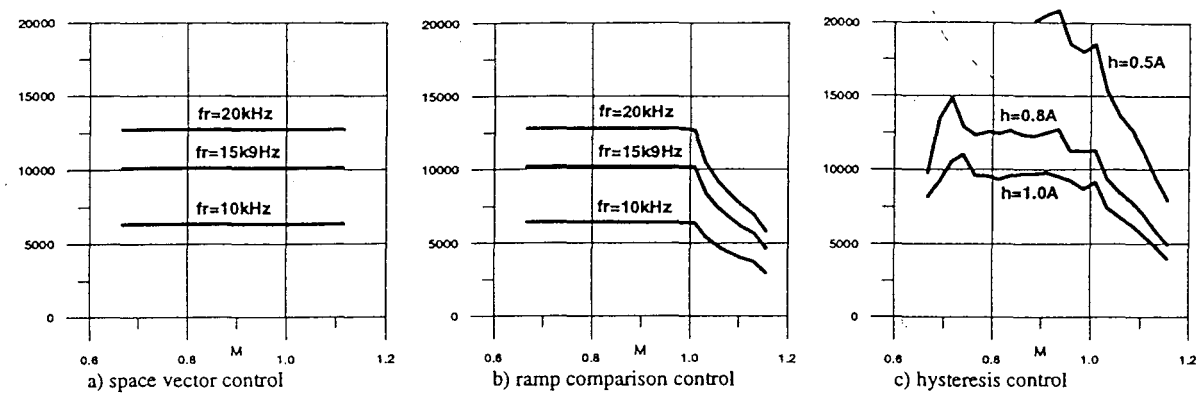

a) space vector control b) ramp comparison control c) hysteresis control

Fig.4: Switching losses of the three control concepts in dependency on M.

$$\underline{u}_U^* = \delta_{(100)}\underline{u}_{U(100)} + \delta_{(000)}\underline{u}_{U(000)} + \delta_{(010)}\underline{u}_{U(010)} + \delta_{(011)}\underline{u}_{U(011)} \quad (8)$$

Using this definition of the modulation index M according to Eq.(9), the relative on-time δ of the switching states (000) and (010) can be calculated directly using simple geometrical relations

$$\delta_{(000)} = \sqrt{3}M\sin\left(\frac{\pi}{3} - \varphi_U\right) - 1, \quad \delta_{(010)} = \sqrt{3}M\sin(\varphi_U) \quad (9)$$

Therefore, we have for the redundant switching states

$$\delta_{(100)} + \delta_{(011)} = 1 - \delta_{(000)} - \delta_{(010)} = 2 - \sqrt{3}\,M\sin\left(\frac{\pi}{3} + \varphi_U\right) \quad (10)$$

In order to minimize the switching frequency of the system we now arrange the switching states within each pulse half period in such a way that the subsequent state can always be obtained by switching of only one bridge leg. With (100) selected arbitrarily as initial switching state we obtain

$$\ldots\Big|_{t=0}(100)\text{-}(000)\text{-}(010)\text{-}(011)\Big|_{t=\frac{1}{2}T_p}(011)\text{-}(010)\text{-}(000)\text{-}(100)\Big|_{t=T_p}\ldots \quad (11)$$

Due to the requirement of a minimum switching frequency one has to reverse the sequence of the voltage space vectors $\underline{u}_{Uj}$ after each pulse half period.

Because of the redundancy of two switching states regarding the generation of $\underline{u}_U^*$ in Fig.2 the sum $\delta_{(100)}+\delta_{(011)}$ can be calculated via Eq.(10) and is therefore fixed, but thereby no specific distribution of the on-times of (100) and (011) is defined. The distribution of the redundant voltage space vectors between begin and end of each pulse half period therefore constitutes a degree of freedom of the modulation method.

The space vector control applied in this paper uses this degree of freedom to minimize the rms value of the harmonics of the input current. Besides this redundancy of the two switching states is also used in a way to make the average value of the neutral point current i_M zero. Otherwise this current i_M would result in a drifting of the neutral point potential and an asymmetry of the output voltages which has to be avoided. The two goals of the space vector control applied in this paper are characterized via

$$\Delta i^2_{N,rms} \rightarrow \text{Min} \quad \text{and} \quad I_{M,avg} = 0 \quad (12)$$

The characteristics of the space vector control are:

+ minimized ripple of the input current
+ constant switching frequency simplifies design of an EMC-filter
+ digital signal processor (DSP) is necessary
+ expensive and difficult realization of the (digital) controller

2. MAINS CURRENT QUALITY

2.1 BASIC CONSIDERATIONS

In this section it is explained how the simulation was carried out to in order to achieve equal switching losses for all the control concepts.

The computer simulations were carried based on the characteristic values: $\hat{I}_N^*$=18A, f_r=15.9kHz, U_O=700V and L=1mH for all values of M.

The ripple of each input current was determined via

$$\Delta i_N = i_N^* - i_N \quad (13)$$

$$i_N^* = u_N \frac{\hat{I}_N^*}{\hat{U}_N} \quad (14)$$

As a quality criterion for the deviation of the input currents from the ideal sinusoidal reference waveform the sum of the squares of the rms values of the current harmonics was chosen according to

$$\Delta I^2_{N,i,rms} = \frac{1}{T_N}\int_{t=0}^{T_N} \Delta i^2_{N,i}\,dt \quad (15)$$

$$\Delta I^2_{ges} = \Delta I^2_{N,R,rms} + \Delta I^2_{N,S,rms} + \Delta I^2_{N,T,rms} \quad (16)$$

As normalization factor we have used

$$\text{norm} = 3\left(\frac{U_O}{8 f_r L}\right)^2 = 90.85\text{A} \quad (17)$$

2.1.1 SPACE VECTOR CONTROL

In case of the space vector control it is easy to calculate the switching losses. As described in [5] the switching losses of a power transistor of the system are proportional to the current being switched in a first approximation. Because of the constant switching frequency f_r and the assumption of a purely sinusoidal shape of the input current with an amplitude $\hat{I}_N$ the losses can be easily calculated via

$$P_{T,P} = \frac{2}{T_N}\int_{t=0}^{T_N/2} k\, i_N\, f_r\, dt = \frac{2}{\pi} k\, f_r\, \hat{I}_N \qquad w_P = k\, i_N \quad (18)$$

(w_p denotes the local switching energy loss of the power transistor).

The switching losses are therefore independent of the modulation index M. Under the assumption of a constant switching frequency f_r and a constant amplitude $\hat{I}_N$ of the input current the switching losses are constant in the whole modulation range M=[0.67 ... 1.15]. The switching losses of the space vector control were taken as a reference value for the comparison of the control concepts (Fig.4a).

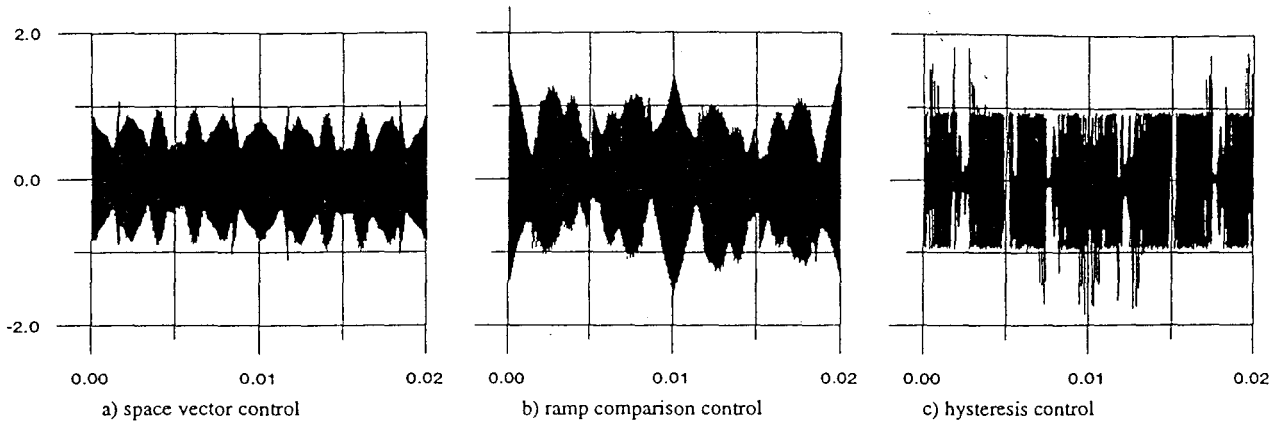

a) space vector control b) ramp comparison control c) hysteresis control

Fig.5: Time behavior of the ripple Δi_N (not normalized) resulting for the three control concepts M=0934 within a mains period.

2.1.2 RAMP COMPARISON CONTROL

As described in section 1.2 for modulation indices M<1 the switching frequency is equal to the frequency of the triangular signal and can therefore be chosen arbitrarily.

So there are we have an identical behavior as in a case of space vector control described above. If the frequency of the triangular signal is selected to be the same as the switching frequency of the space vector control the switching losses are equal for all M<1 (Fig.4b).

It is important to point out that this is only the case for M<1. In the region of overmodulation M>1 the switching frequency is different from the frequency of the triangular signal (as explained in section 1.3). In that case a few simulation runs had been necessary. The frequency of the triangular signal was changed as long as the measured switching losses were different from the reference switching losses of the space vector control. In the long run the frequency of the triangular signal was found for every M. Because of low order harmonics appearing for M>1, overmodulation is not applied for rectifier systems and therefore not examined in detail in this paper.

2.1.3 HYSTERESIS CONTROL

For hysteresis control the switching frequency is not constant, but dependent on the width h of the hysteresis band and also on the modulation index M.

In order to make the switching losses equal to the switching losses of the space vector control it was necessary to perform several simulation runs for every value of M trying different values of h. So it was possible to find the width h for every value of M according to the reference switching losses of space vector control.

2.1.4 INFLUENCE OF THE CONTROL PARAMETERS

The effects of the control parameters on the switching losses are shown in Fig.4. In case of space vector control the switching losses are constant and dependent on the arbitrarily chosen switching frequency (Fig.4a). In Fig.4b the switching losses for three different frequencies for the ramp comparison control are shown. In case of overmodulation M>1 the switching losses decrease if the frequency is held constant. Fig.4c shows the dependency of the switching losses on the modulations index and on the width of the hysteresis band for hysteresis control.

2.2 RIPPLE OF THE INPUT CURRENTS

The simulations were carried out as explained in the previous section, the results are presented in the following.

In **Fig.5** the time behavior of the ripple resulting for the three control concepts is shown for M=0.934 (a realistic value in case of a practical realization of the system). There, the ripple is not normalized.

Figure 6 shows the resulting local total rms value of the ripple

$$\Delta i^2_{N,rms} = \Delta i^2_{N,R,rms} + \Delta i^2_{N,S,rms} + \Delta i^2_{N,T,rms} \qquad (19)$$

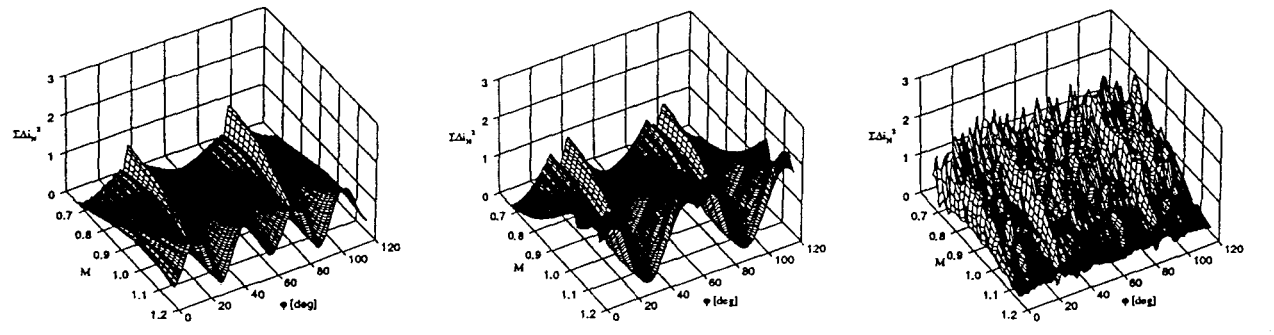

a) space vector control b) ramp comparison control c) hysteresis control

Fig.6: Average local rms-values of the total ripple (Eq.(19)) in dependency on the modulation index M and the position φ_U of a pulse interval within a mains period.

of the input current of the system for $\varphi_U = \in [0 .. 2\pi/3]$ where

$$\Delta i^2_{N,i,rms} = \frac{2}{T_P} \int_{\mu=0}^{\mu=T_P/2} \Delta i^2_{N,i} d\mu_t \qquad i = R,S,T \cdot \tag{20}$$

In order to determine a kind of local average characteristic of the ripple, for the sum of the ripples of the three phases shown in Fig.6 all harmonics having a frequency higher than f_k=5kHz are neglected.

According to Fig.6 for hysteresis control the ripple is very small for high modulation index M, while it is high for low values of M. In case of hysteresis control (Fig.6c) the chaotic behavior is obvious in form of sharp peaks in the surface, although these peaks are smoothened by the filtering described above. Fig.6a and Fig.6b show the ripple characteristics for space vector control and ramp comparison control. Different to hysteresis control the ripples are high for high modulation index M. In Fig.6b for a modulation index M>1 the case of overmodulation is shown in form of a sharp decline of the surface (as explained in section 1.3).

To compare the rms values of the ripples resulting for the three control concepts the currents are integrated according to Eq.(15). The results are shown in Fig.7 where the global rms values of the ripples of the control concepts can be compared to each other directly in dependency on the modulations index M.

Surprisingly the ripple of the hysteresis control is lower even than for optimum space vector control, what is possible because of the not constant switching frequency in case of the hysteresis control. By using a non-sinusoidal pre-control signal the mains current quality of ramp comparison control could reach values as nearly as good as given for space vector control. So the current quality of space vector control can be seen as the minimum which could be reached using ramp comparison control with optimized pre-control.

3. SPECTRA OF THE MAINS CURRENT

In a practical realization of the system it is necessary to insert an EMC-filter between the AC-terminals of the rectifier and the mains. Therefore, not only the ripple of the input current but also the spectrum of the harmonics of the input current has to be taken into account when the effects of a control concept on the mains are investigated. The following sections deal with this important aspect.

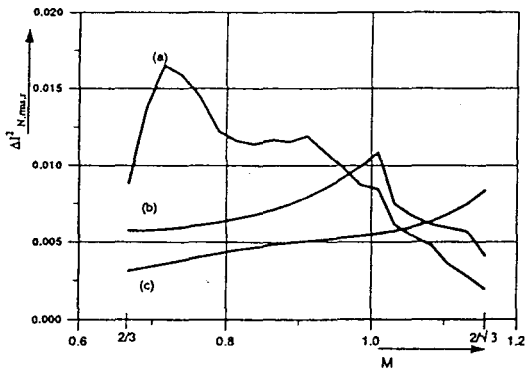

Fig.7: Comparison of the normalized harmonic losses $\Delta I^2_{N,rms,r}$ for hysteresis control (a), ramp comparison control (b), and space-vector based harmonic-optimal continuous modulation (c) in dependency on the modulation index M.

3.1 CALCULATION OF THE CURRENT SPECTRA

For calculating a spectrum the Fourier analysis is performed according to

$$f(t) = \frac{A_0}{2} + \Sigma\left(A_n \cos(\omega_N t) + B_n \sin(\omega_N t)\right) \tag{21}$$

where

$$A_n = \frac{2}{T_N} \int_{t=0}^{T_N} f(t)\cos(\omega_N t)dt \qquad B_n = \frac{2}{T_N} \int_{t=0}^{T_N} f(t)\sin(\omega_N t)dt$$

This only holds in case of a function f(t) which is strictly periodic with period T_N.

Especially in case of hysteresis control the spectrum of the input current and/or of the ripple of the input current changes within each period because of the chaotic behavior being characteristic for hysteresis control. Also the spectra of the currents of the three phases R, S, T are different from each other. In order to achieve only a single characteristic spectrum which can be used for a comparison, the following was done:

A simulation run was performed over a large number of periods (21 periods) and the input currents of the three phases R, S, T were measured. For some periods (the 5th, the 10th, the 15th and the 20th) the harmonics were calculated according to Eq.(21). This results in a number of spectra (12 different spectra) that look all a little bit different according to the inexactness of the periodicity which is inherent with the hysteresis control. After that the average of the harmonics of the 12 spectra was formed

$$c_{n,avg} = \sqrt{\frac{1}{12}(c^2_{n,1} + c^2_{n,2} + \ldots + c^2_{n,12})} \cdot \tag{22}$$

$c_{n,1}$ ... n^{th} harmonic of the spectrum 1,
$c_{n,2}$ ... n^{th} harmonic of the spectrum 2, etc.
$c_{n,avg}$ ... n^{th} harmonic of the averaged spectrum.

This resulted in a single averaged spectrum which is used in the following section for the comparison of the spectra of the three different control concepts. The amplitude of the averaged harmonic $c_{n,avg}$ represents the averaged power of the harmonic with ordinal number n.

The procedure described above was performed not only for hysteresis control but also for ramp comparison control and space vector control. Because for ramp comparison control and especially space vector control the inexactness of the periodicity of the ripples is very small, there the averaged spectrum is not very different from the single spectrum.

3.2 COMPARISON OF THE SPECTRA

For a specific value of the modulation index M=0.934, which is realistic for a practical realization of the rectifier, the spectra of the ripple of the input currents are calculated for the three different control concepts. The results are shown in Fig.8, where Fig.8a shows the spectrum for the space vector control, Fig.8b the spectrum of the ramp comparison control, and Fig.8c the spectrum resulting for hysteresis control.

For the spectrum of the space vector control and the ramp comparison control the harmonics are pronounced at multiples of the switching frequency. Considering low-order harmonics the space vector control gives lower amplitudes than ramp comparison control. The spectrum of the hysteresis control is quite different. There are no peaks of specific harmonics. This is due to the variation of the switching frequency being characteristic for hysteresis control (section 1.2).

Figure 9 shows the effect of a 2nd-order EMC-Filter according to Eq.(23), which is connected in series on the mains side. While the switching frequency of the ramp comparison control and the space

vector control is f_t=15.9kHz, the cut-off frequency of the filter is chosen to be f_{filt}=5kHz. For the transferfunction of the filter we have

$$\frac{i_N}{i_U} = \sqrt{\frac{1+\left(\omega \frac{L_F}{R_F}\right)^2}{\left(1-\left(\frac{\omega}{\omega_F}\right)^2\right)^2 + \left(\omega \frac{L_F}{R_F}\right)^2}} \qquad (23)$$

$$\omega_F = \frac{1}{\sqrt{L_F \cdot C_F}} \quad f_{filt} = \frac{\omega_F}{2\pi} = 5\text{kHz} \quad \frac{L_F}{R_F} = \frac{1}{50000}$$

C_F ... capacitor of the filter
L_F ... input side inductance
RF ... resistor connected in parallel to LF

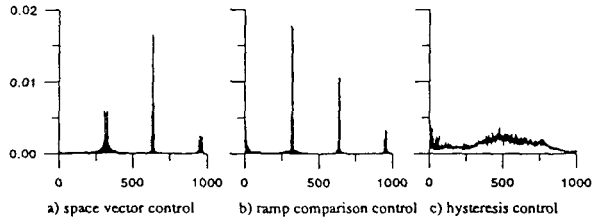

Fig.8: Comparison of the normalized input current spectra (related to the fundamental).

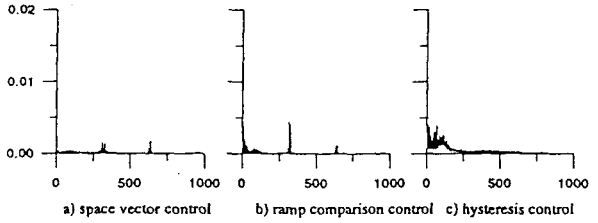

Fig.9: Comparison of the normalized mains current spectra of the different control concepts resulting for a 2nd-order EMC-Filter being inserted between rectifier system and mains.

4. STRESS ON THE OUTPUT CAPACITORS

The two output capacitors (which in general are realized as electrolytic capacitors) have to be dimensioned with respect to the rms current stress and admissible (low-frequency) ripple of the neutral point potential u_M. In order to not exceed a given maximum value of the amplitude $\hat{U}_{M,(k)}$ of a change of the capacitor voltage (as caused by the low-frequency harmonics $\hat{I}_{M,(k)}$ of the neutral point current) we have to select:

$$C \geq \frac{\hat{I}_{C,(k)}}{k\,\omega_N\,\hat{U}_{C,(k)}} \qquad (24)$$

($\hat{U}_{M,(k)}$ is typically set to 0.01 U_O) There k denotes the order of the current and voltage harmonics with respect to the mains frequency. For constant total output voltage U_O (controlled with high dynamics) a parallel connection of the output capacitors exists concerning the harmonics of the current i_M flowing into the neutral point M. Therefore, the center point current harmonics are divided into equal parts in both output capacitors. They shift the potential of the neutral point, but do not change the total output voltage U_O. Therefore, the harmonics of a capacitor current are to be calculated from the harmonics of i_M via $\hat{I}_{C,(k)} = ½\,\hat{I}_{M,(k)}$

The dependency of the amplitudes of the low-frequency harmonics k=3 and k=9 (which are of special importance for dimensioning) on the modulation index M for the three different control concepts is shown in **Fig.10**. The amplitudes of the harmonics are normalized to the amplitude of the input current fundamental.

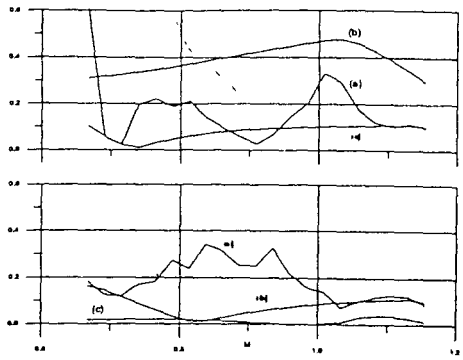

Fig.10: Normalized amplitudes of the 3rd (top) and 9th (bottom) harmonic of the neutral point current i_M for hysteresis control (a), ramp comparison control (b) and space vector control (c) in dependency on the modulation index M.

As Fig.10 shows the harmonics of the neutral point current resulting for space vector control are much smaller than for the other two control concepts. There is also only a small dependency on the modulation index M.

Especially the hysteresis control shows a significant dependency of the amplitudes of the harmonics on the modulation index M. For example, for M=0.9 the third harmonic of the neutral point current is reduced to about zero. Compared to the ramp comparison control the hysteresis control shows some advantages in a wide region of the modulation index M.

5. CONCLUSIONS

The paper compares the influence on the quality of the input currents of three well known control concepts which are applied on a three-phase/switch/level PWM (VIENNA) rectifier system. It is shown that there is a strong dependency on the modulation index M.

For low values of M the ripple according to hysteresis control is much higher than for ramp comparison control or space vector control. In the region M>1 the ripple of the hysteresis control becomes relatively small, even smaller than for ripple-minimized space vector control (witch constant switching frequency). Also the spectrum of the input current shows very low amplitudes in case of hysteresis control as compared to ramp comparison control or space vector control. While the amplitudes of the low-frequency harmonics of the neutral point current is rather low for space vector control, hysteresis control shows a strong dependency on the modulation index M, but still gives better results than ramp comparison control.

6. REFERENCES

[1] **Kolar, J. W., and Zach, F. C.:** *A Novel Three-Phase Three-Switch Three-Level PWM Rectifier.* Proceedings of the 28th Power Conversion Conference, Nürnberg, Germany, June 28-30, pp. 125-138 (1994).

[2] **Nagy, I.:** *Improved Current Controller for PWM Inverter Drives with the Background of Chaotic Dynamics.* Proceedings of the 20th International Conference on Industrial Electronics, Control and Instrumentation, Bologna, Italy, Sept. 5-9, Vol. I, pp. 561-566 (1994).

[3] **Kolar, J. W., Drofenik , U., and Zach, F. C.:** *Space Vector Based Analysis of the Variation and Control of the Neutral Point Potential of Hysteresis Current Controlled Three-Phase Three-Switch Three-Level PWM Rectifier Systems.* Proceedings of the International Conference on Power Electronics and Drive Systems, Singapore, Feb. 21-24, Vol. 1, pp. 22-33 (1995).

[4] **Mohan, N., Undeland, T. M., and Robbins, W. P.:** *Power Electronics: Converters, Applications and Design.* New York: John Wiley & Sons Inc., 2nd Edition (1995).

[5] **Kolar, J. W., Ertl, H., and Zach, F. C.:** *Design and Experimental Investigation of a Three-Phase High Power Density High Efficiency Unity Power Factor PWM Rectifier Employing a Novel Power Semiconductor Module.* Proceedings of the 11th IEEE Applied Power Electronics Conference, San Jose (CA), USA, March 3-7, Vol. II, pp. 514-523 (1996).